1

2
3
4
5   Supplemental Information for

6   Thompson, L.G., *et al*.

7   Ice Core Records of Climate Variability on the Third Pole

8   with Emphasis on the Guliya ice cap, western Kunlun Mountains

9
10
11   Figures S1 to S7
12
13
14
15
16
17
18
19
20
21
22
23
24
25
26
27
28
29
30
31
32
33
34
35
36
37
38
39
40
41
42
43

44
45
46
47
48
49
50
51
52
53
54
55
56
57
58
59
60
61
62
63
64
65
66
67
68
69
70
71
72
73
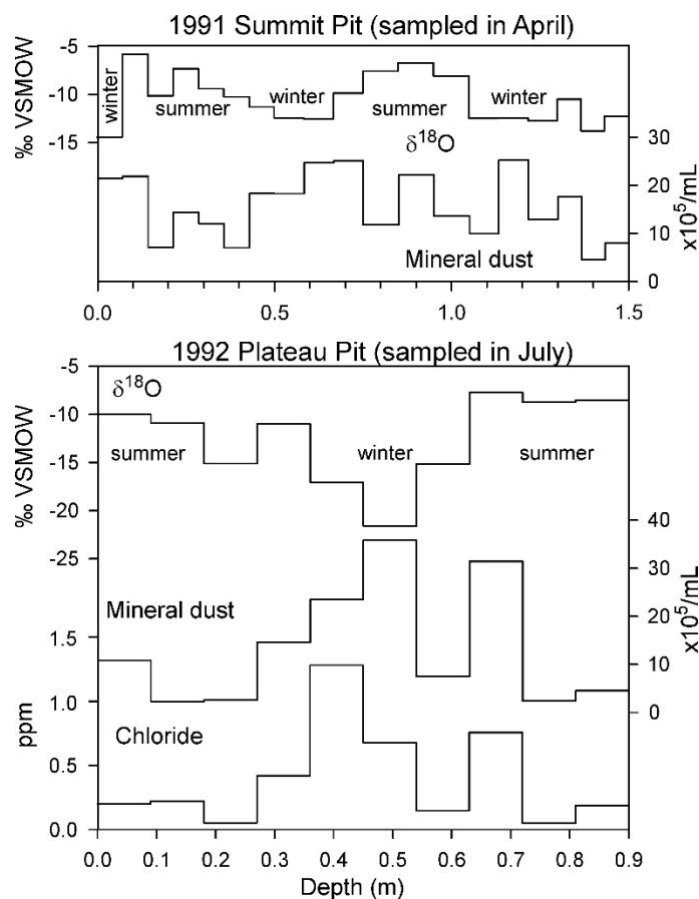
74 **Figure S1.** Top: A pit excavated to 1.5 m on the summit in April 1991 shows two annual cycles in $\delta^{18}O$, although
75 the seasonal variations in dust are poorly defined. However, this may be due to the handling of the samples which
76 were melted and bottled at the field site and thus were more vulnerable to contamination.

77
78 Bottom: Analysis of pit samples taken at the plateau drill site in 1992 demonstrates seasonal variations in $\delta^{18}O$,
79 mineral dust and chloride concentrations such that the most depleted isotopes occur in the winter and the highest
80 concentrations of aerosols occur in the late winter to early spring. This pit contained snow and firn throughout,
81 and the bottom of the pit marks the abrupt firn/ice transition.
82
83
84
85
86
87
88
89
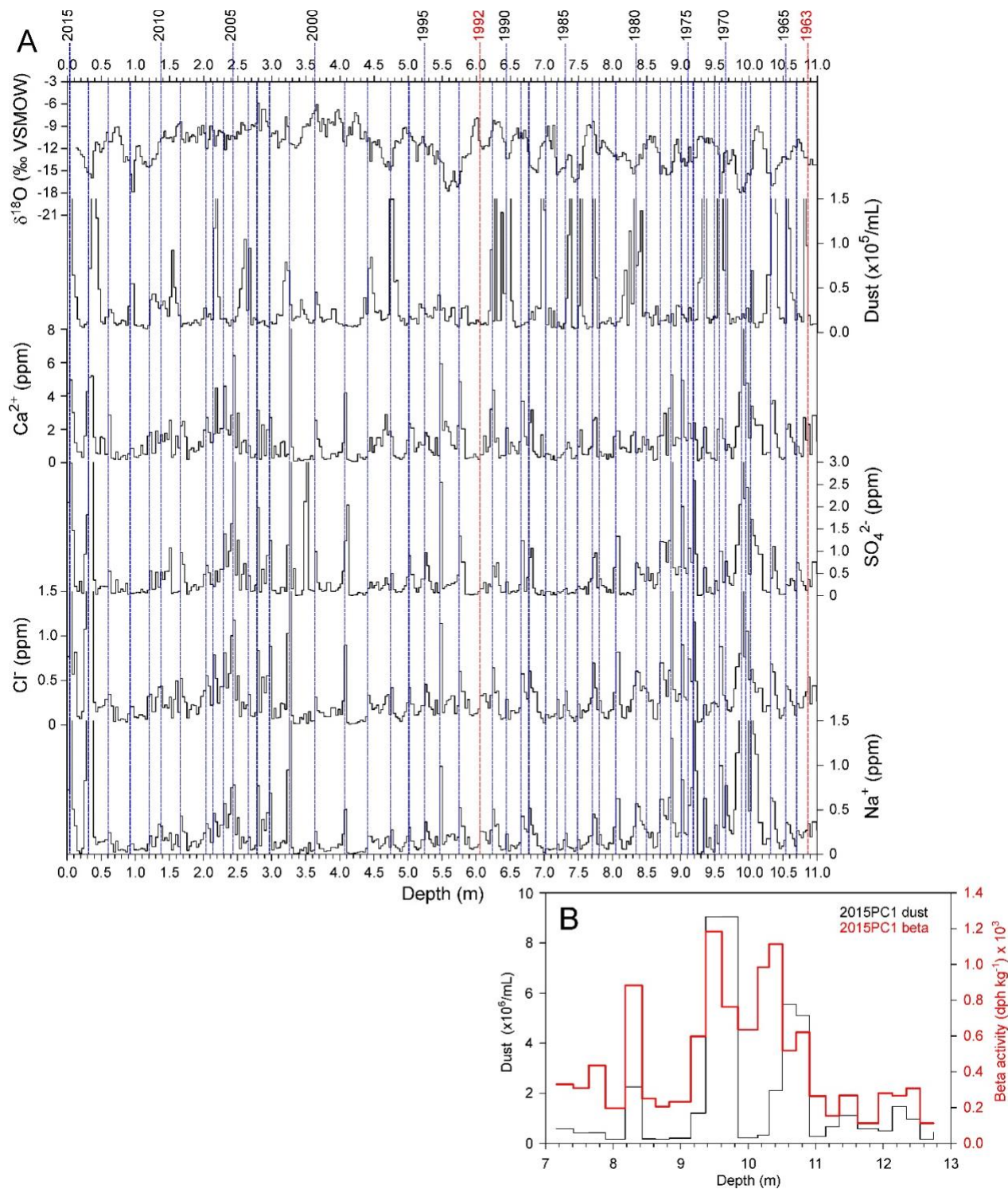
Figure S2. (A) Time scale development for the top 11 meters of 2015PC1. Known time horizons at 1992 and 1963 are marked in red. (B) Beta radioactivity (red plot) and dust concentrations (black plot), calculated at the same depth intervals as beta. Note that the depth scales for (A) and (B) are aligned.

Because of the extremely low snow accumulation rate, annually resolved time scale construction of the climate record is much more difficult than for the Dasuopu ice core in the high-accumulation

97 region of the central Himalaya (Thompson *et al.,* 2000). Although the seasonal variations in $\delta^{18}O$ in fresh
98 snow at both sites and the aerosol variations on the plateau are well defined, these oscillations are less
99 discernible in the firn and ice in the summit cores and in the ice in the plateau cores (which are
100 composed of ice below the top meter). In order to construct an annual time series (Fig. S2A), the two
101 fixed horizons (red lines) at 1992 (at 6 m) and 1963 (at 10.9 m depth determined by beta radioactivity
102 emission analysis) (Fig. S2B) in 2015PC1 are used to calibrate the time scale. The fixed point at 1992 is
103 determined by matching the $\delta^{18}O$ data in the 2015PC1 and 1992PC records (Fig. 4A, main text).
104 According to this isotopic match, the top of the 1992 record lines up with the 2015 core at 6 meters.
105 Usually the peak in beta activity is associated with the intense 1962/63 Soviet thermonuclear testing in
106 the Arctic; however, in the case of 2015PC1 peak, beta occurs with very high dust concentrations (Fig.
107 S2A). Radionuclides such as ^{90}Sr and ^{137}Cs, when emitted into the atmosphere, attach to dust particles
108 (Igarashi *et al*., 1996). Since the variations in the beta activity follow the dust concentration variations,
109 we assume that the point at which the radioactivity rises above background (10.9 m) marks 1962/63.
110   Parameters used for annual signals were chosen as representatives of potential aerosol source
111 types (Cl^- and Na^+ are typical of salts, dust and Ca^{2+} have crustal origins, and SO_4^{2-} may originate from
112 salts or volcanic emissions). Oxygen isotopic ratios should vary seasonally, but may have been altered by
113 post-depositional processes. Correlation coefficients (R) between $\delta^{18}O$ and Cl^-, Na^+ and Ca^{2+} range from -
114 0.22 to -0.24 (p<0.01, N=588) between 10 and 30 m. Correlation coefficients were not calculated above
115 10 m because dust and major ion samples are not co-registered. The determination of a year is based on
116 matching peaks between at least three of these six parameters. For example, the large SO_4^2 peak at 3.5
117 m is not considered to be an annual layer because it is not supported by any of the other major ions,
118 although a minor peak in mineral dust occurs at that depth.
119   A time scale was developed for 2015PC2 in an identical manner to that for 2015PC1. However,
120 because of dating uncertainties resulting from the low accumulation and post-depositional processes,
121 the time series of the two GP cores display increasing offsets below the 1962/63 calibration point. Thus,
122 averaging the independently dated time series would cause distortion of the record below the 1960s.
123 Therefore, below 1962 the raw $\delta^{18}O$ data from 2015PC2 are matched to the 2015PC1 $\delta^{18}O$ data, and the
124 time scale from the latter is transferred to the former. Figure S3A shows the time/depth relationships in
125 all the cases described above: the 2015PC1 and 2015PC2 time scales which were developed by
126 independent annual layer counting, and the 2015PC2 time scale below 1962 which was developed by
127 isotopic matching to 2015PC1. The differences between the two 2015PC2 time scales below 1962
128 (corresponding to 12.5 m) are shown in Fig. S3B, and are taken as the range of uncertainty in dating
129 precision between the two GP cores.

130 **Reference**

131 Igarashi, Y., Otsuji-Hatori, M., Hirose, K., 1996. Recent deposition of ^{90}Sr and ^{137}CS observed in Tsukuba.
132 *J. Environ. Radioactivity* 31, 157-169.
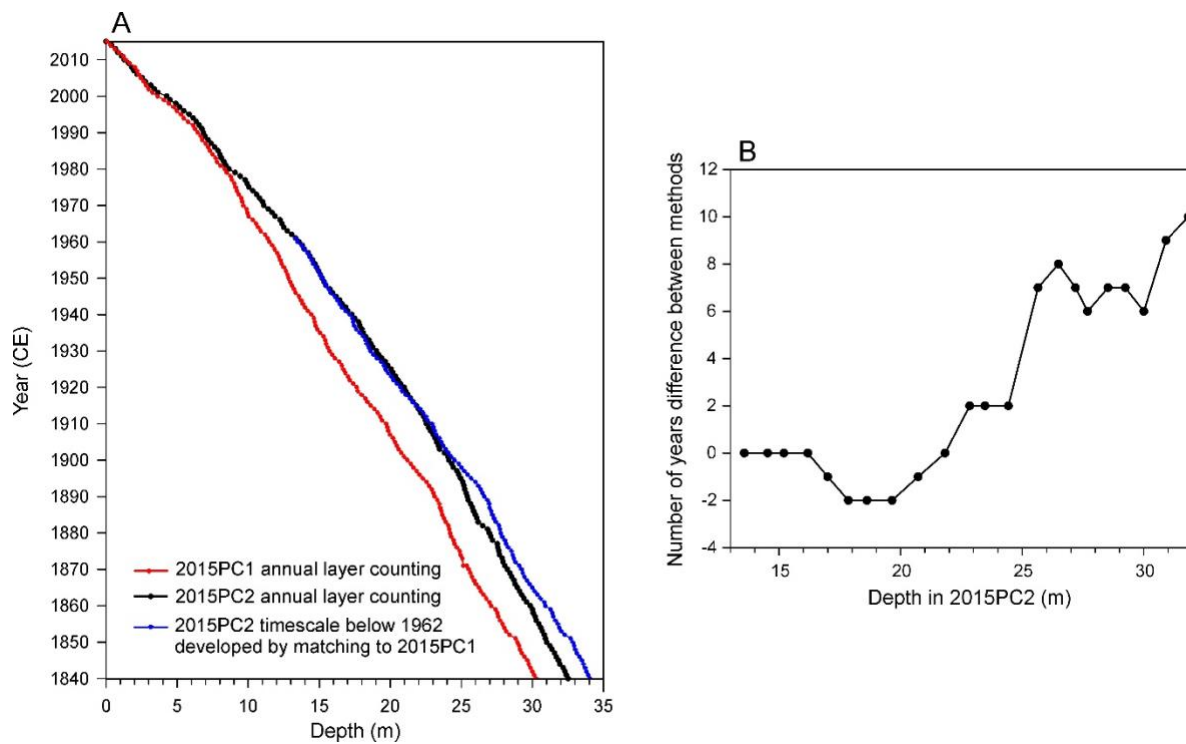
Figure S3. (A) Time vs. depth relationships in 2015PC1 and 2015PC2 cores. (B) Range of dating uncertainty (every five years) between the GP cores based on the age difference between layer counting in 2015PC2 and time scale transfer from 2015PC1 to 2015PC2 below 1962 CE.
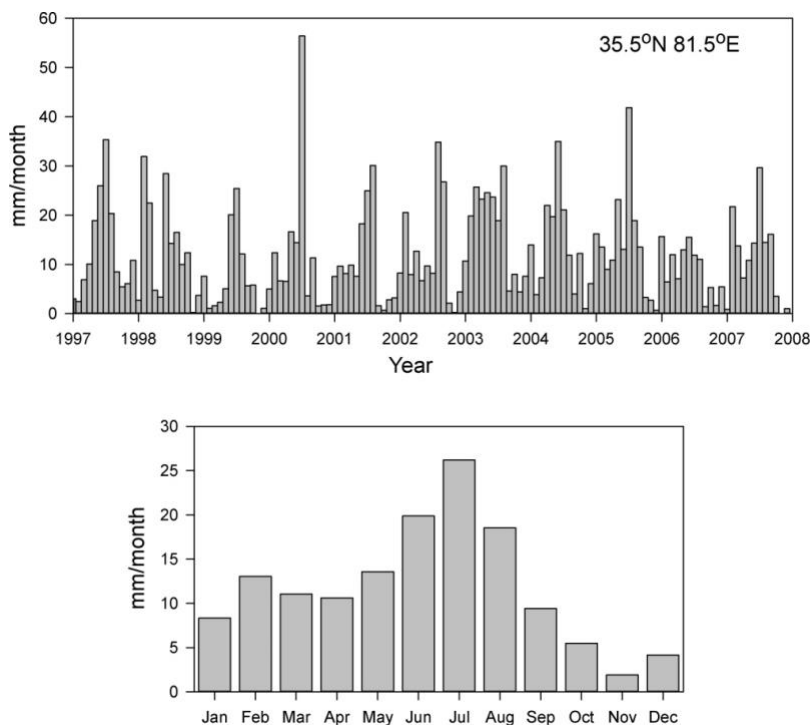
142

143   **Figure S4.** The seasonal precipitation distribution in the vicinity of the Guliya ice cap, as shown by GPCP monthly
144   data from 1997 to 2007 (top) and by the monthly climatology for this period (bottom). Approximately 45% of
145   annual precipitation falls from June to August, 12% from September to November, 18% from December to
146   February, and 25% from March to May. Thus, this area receives nearly equal amounts of precipitation during the
147   pre-monsoon and monsoon seasons.

148

149
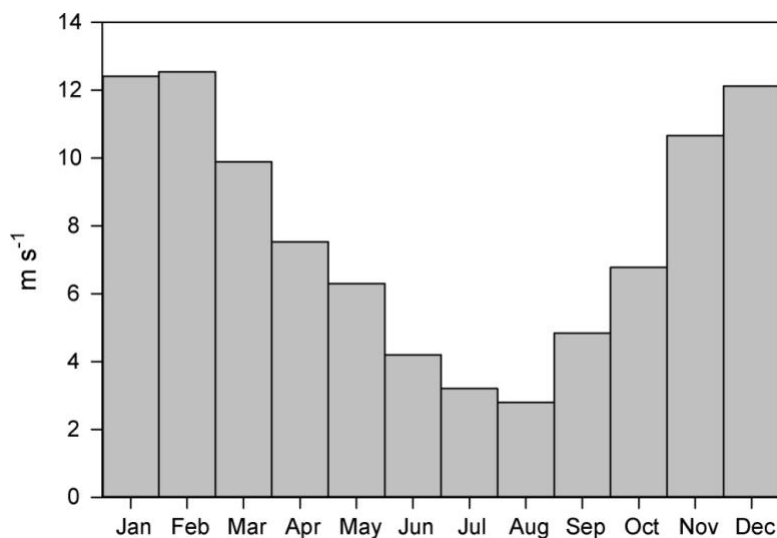
150
151

152

153   **Figure S5.** Average (from 2005 to 2016) monthly zonal wind velocities at 500 hPa to the west of, and over, the
154   Guliya ice cap (40°N to 30°N; 70°E to 85°E). Data are from http://iridl.ldeo.columbia.edu/SOURCES/.NOAA/.NCEP-
155   NCAR/.CDAS-1/.MONTHLY/.Intrinsic/.PressureLevel/.u/

156
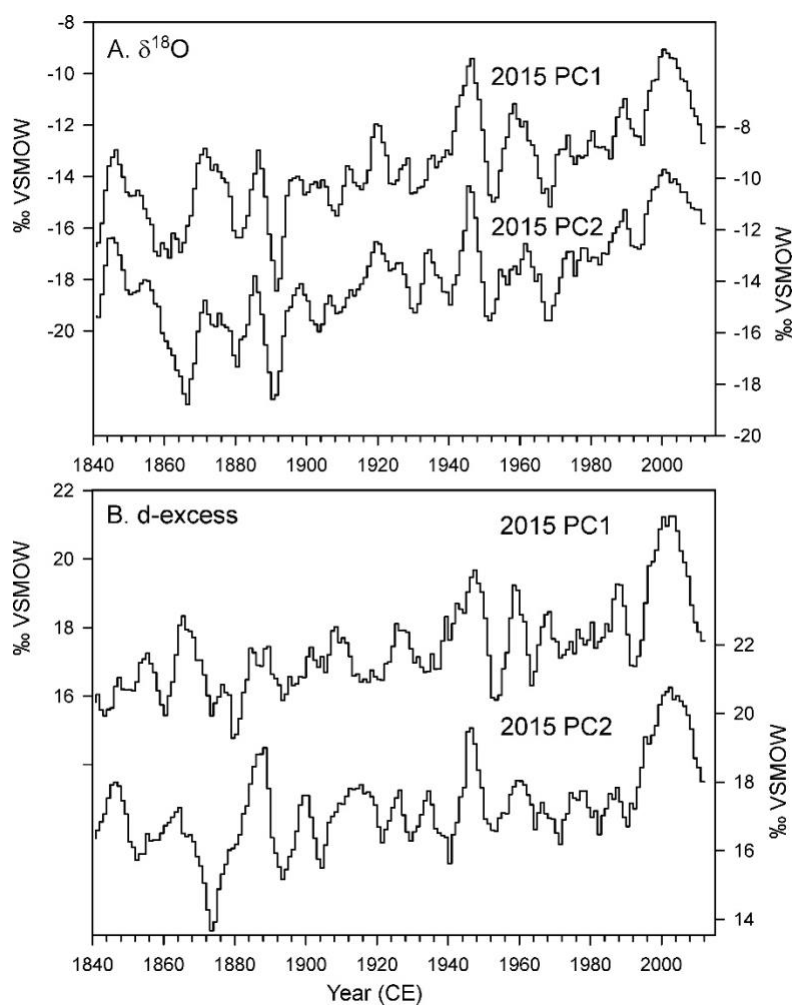
157

158

159   **Figure S6.** Five-year running means of (A) $\delta^{18}O$ and (B) deuterium excess records from Plateau Core 1 (2015PC1)
160   and Plateau Core 2 (2015PC2).

161

162
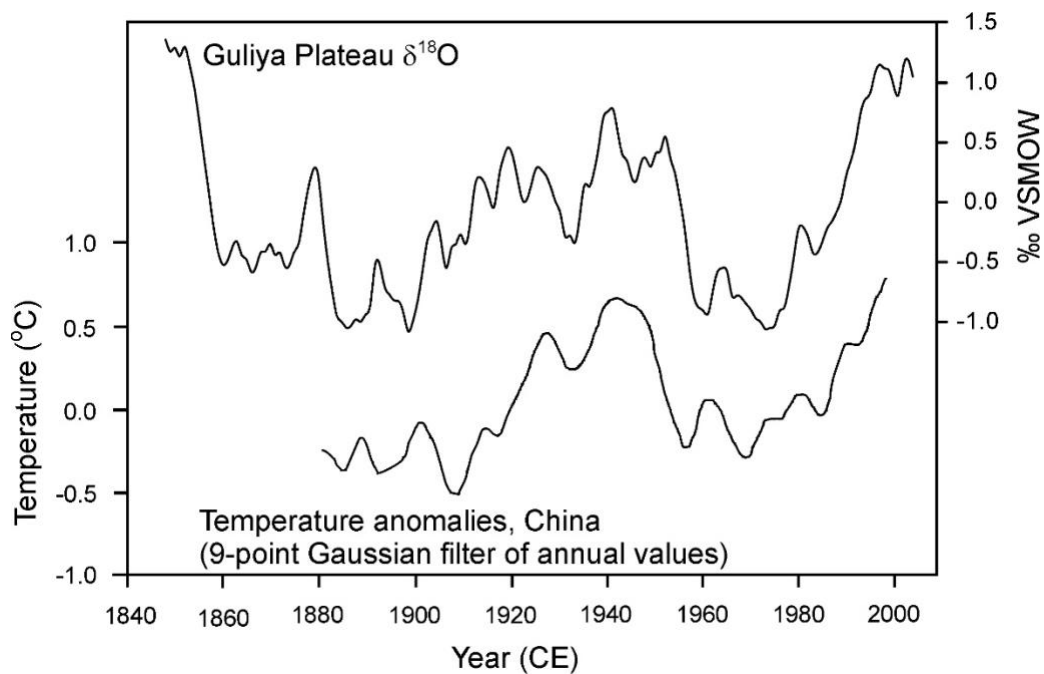
Figure S7. Comparison of δ¹⁸O record from the Guliya Plateau ice cores (2015PC1 and 2015PC2 combined) and temperature anomalies for China as a whole, including the Third Pole region. The Guliya δ¹⁸O record is detrended and smoothed with 19-year running means, and the China temperature record is adapted from Wang and Gong (2000, Fig. 1b) by manual tracing of the spline curve in the figure.

163
164
165
166

167

168

169